Thermal-hydraulic Prediction for Wet Region of Economizer Using Spirally Finned Tubes

Masahiro OSAKABE* and Tugue ITOH*

In order to improve the boiler or thermal plant efficiency, latent heat recovery from the flue gas is very important concept. Condensation heat transfer on horizontal spirally finned tubes of fin pitch 5 and 10mm was investigated experimentally by using an actual flue gas from a natural gas boiler. The experiments were conducted at different steam mass concentrations of the flue gas and a wide range of tube wall temperature. The mass concentration was controlled with a steam injection into the flue gas. Fin efficiency at the condensation region was significantly lower than that at the dry region. The empirical correlation developed for a single-phase fluid was extrapolated to the condensation heat transfer region. The fin efficiency was evaluated with an equivalent heat transfer coefficient used as a first approximation. The heat and mass transfer behaviors on the spirally finned tube were well predicted with the analogy correlation based on the empirical correlation. The obtained correlation was incorporated into the prediction code and verified with the economizer experiments. The experimental results for the temperature distributions of water and flue gas agreed well with the prediction.

Keywords: Boiler, Actual flue gas, Heat and mass transfer, Condensation

1. INTRODUCTION

The most part of energy losses in boiler or thermal plant is due to the heat released by the exhaust flue gas to atmosphere. The released heat consists of sensible and latent one. Recently, for a biological and environmental safety, a clean fuel such as a natural gas is widely used in the boiler or power plant. As the clean fuel includes a lot of hydrogen instead of carbon, the exhaust flue gas includes a lot of steam accompanying with the latent heat. So the latent heat recovery from the flue gas is very important to improve the system efficiency.

For the latent heat recovery from a boiler, condensation heat transfer experiments[1-3] have been conducted by using steam-air mixtures. These experiments yield different opinions on the analogy for heat and mass transfer. Furthermore, condensation in actual flue gas is more complex and least understood. So it was difficult to predict the accurate thermo-fluid behavior of an actual condensing heat exchanger using an actual flue gas. Condensation heat transfer on horizontal spirally finned tubes of fin pitch 5 and 10mm was investigated experimentally by using the actual flue gas from a natural gas boiler. The experiment was conducted at different air ratios and steam mass concentrations of the flue gas in a wide range of tube wall temperature.

Thermal-hydraulic behavior of economizer for the latent heat recovery was investigated experimentally by using an actual flue gas from a propane gas fuel boiler. Two kinds of countercurrent cross-flow heat exchangers, which consist of spirally finned tubes of fin pitch 5 and 10mm, were designed and used for the experiment. Based on the above basic studies, a prediction method for the economizer was proposed. In the prediction, the flue gas was treated as a mixture of CO_2, CO, O_2, N_2 and H_2O, and the one-dimensional heat and mass balance calculation along the flow direction of flue gas was conducted. The heat and mass transfer on tubes was evaluated with the simple analogy correlation.

*Tokyo University of Mercantile Marine
2-1-6 Etchujima, Koutou-ku, Tokyo 135-8533, Japan
Phone & FAX +81-3-5245-7404
E-Mail osakabe@ipc.tosho-u.ac.jp

The fin efficiency at the condensing region was calculated with a semi-empirical correlation obtained in the basic study.

2. NOMENCLATURE

A: heat transfer area[m^2]
C: mass concentration per fluid of a unit volume [kg/m^3]
C_p: specific heat [kJ/kg]
d: outer diameter of base tube [m]
d_i: inner diameter of base tube [m]
D: mass diffusivity(m^2/s)
h_V: heat transfer coefficient [$kW/(m^2K)$]
h_C: mass transfer coefficient [m/s]
L_W: latent heat [kJ/kg]
L_F: fin height[m]
m_S: injected steam flow rate [kg/s]
Nu: Nusselt number($= h_V d / \lambda$)
P: pressure [Pa]
q: heat flux [kW/m^2]
Pr: Prandtl number($= \nu / \kappa$)
Re: Reynolds number($= ud / \nu$)
R: relative humidity of air
S_F: fin space[m]
Sh: Sherwood number ($= h_C d / D$)
Sc: Schmidt number ($= \nu / D$)
T: temperature [°C]
t_F: thickness of fin plate[m]
u: velocity at minimum flow area [m/s]
V: volumetric flow rate [m_N^3/s]
w: mass concentration per fluid of an unit mass [kg/kg]
η: fin efficiency
κ: thermal diffusivity ($= \lambda / (\rho C_P)$)
λ: heat conductivity [W/(mK)]
μ: air ratio
ν: kinematic viscosity [m^2/s]
ρ: density [kg/m^3]
subscript
a: atmosphere, C: condensation, COX: carbon dioxide and monoxide, d: dry gas, F: fuel, f: flue gas, V: convection, W:

wall, N: standard condition at 0°C and atmospheric pressure, sat: saturated condition of steam, sub: subcooling, wt: wet gas

3. SINGLE STAGE TUBE EXPERIMENT

3.1 EXPERIMENTAL APPARATUS AND METHOD

Shown in Fig.1 is a schematic of experimental apparatus. The flue gas from a natural gas test boiler was cooled from 270°C to 120~200°C by a heat exchanger without the condensation. The steam and SO_2 concentrations in the flue gas can be controlled with steam and SO_2 injections systems upstream of the test section. The steam was supplied from another steam boiler and measured with a vortex-shedding flow meter. The error was within ±2% of the measured value. The flow rate and pressure of the natural gas fuel supplied to the test boiler were measured. The error of the flow rate was within ±0.5%. The flue gas temperatures just above and below the test tubes were measured with sheathed K-type thermocouples of 0.5 mm in diameter.

A water cooled test tube with spiral fin of SUS304 was installed in a transparent polycarbonate duct with the cross-section of 160mm×101mm as shown in Fig.2.

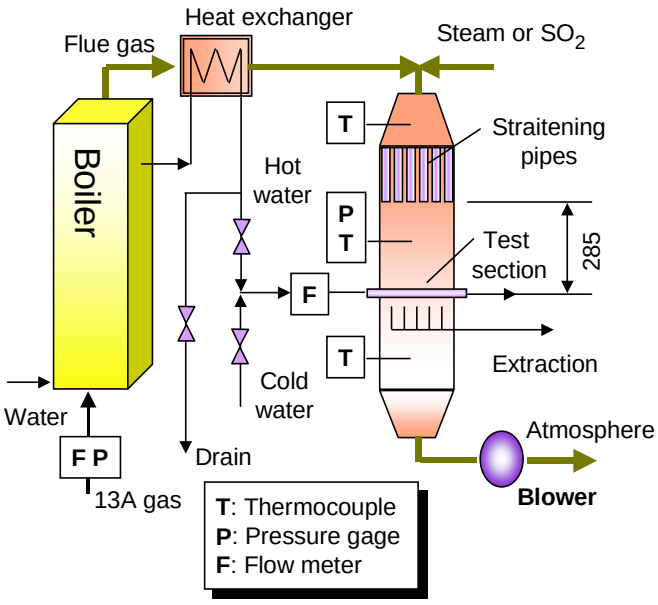

Fig. 1 Schematic of experimental apparatus

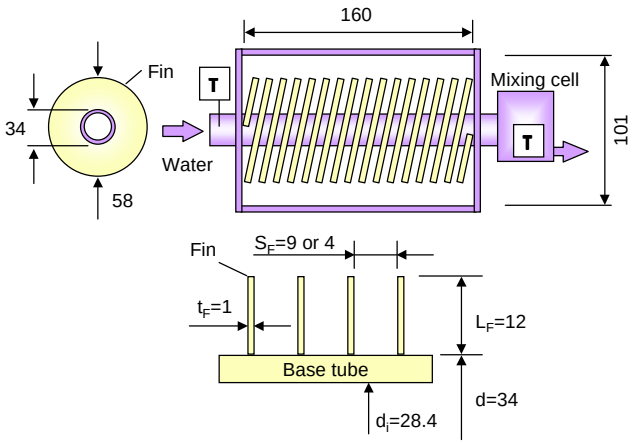

Fig. 2 Test section of spirally finned tube

The water flow rate was measured with a turbine flow meter within an error of ±2%. The inlet and outlet water temperatures of the test tubes were measured also with the sheathed K-type thermocouples of 0.5 mm in diameter. The outlet temperature was measured at a mixing chamber to obtain a well-mixed bulk temperature. The temperature difference of the cooling water through the test tubes was kept approximately at 1~4 K. The heat flux of the test tubes was calculated with the flow rate and the temperature difference of cooling water through the tubes. The measurement error of the heat flux was estimated to be 20% as the maximum in the non-condensation region and 5% as the minimum in the condensation region. The thermocouple signals were transferred to a personal computer with a GPIB line and analyzed. The measurement error of the temperature in this study was within ±0.1 K.

Table1. Composition of natural gas fuel(13A)

CH_4	88.0 %
C_2H_6	5.8
C_3H_8	4.5
C_4H_{10}	1.7

The composition of natural gas fuel used in the test boiler is shown in Table.1. Volumetric concentrations of N_2, CO_2, O_2 and CO in the dry gas were measured by a gas analyzer. The measurement error was within ±10 % for CO_2, within ±0.7 % for O_2 and within ±15 % for CO. By using the measured concentration, the air ratio μ is calculated as

$$\mu = \frac{N_2}{N_2 - \frac{0.79}{0.21}(O_2 - 0.5 \cdot CO)} \quad (1)$$

The molar fraction of the carbon in the fuel of 1 mol can be calculated as,

$$CCR = 1 \times 0.88 + 2 \times 0.058 + 3 \times 0.045 + 4 \times 0.017 \quad \text{mol}$$

By using the volumetric flow rate of the fuel V_F, the volumetric flow rate of the carbon dioxide and monoxide, V_{COX} , is

$$V_{COX} = V_F \cdot CCR \quad (2)$$

The volumetric flow rate of dry gas V_d is,

$$V_d = \frac{V_{COX}}{CO_2 + CO} \quad (3)$$

The molar fraction of the hydrogen corresponding to CO_X of 1 mol can be calculated as,

$$CHR = (4 \times 0.88 + 6 \times 0.058 + 8 \times 0.045 + 10 \times 0.017) / CCR \quad \text{mol}$$

Considering that the air flow rate necessary for the combustion of the fuel is $V_d N_2/0.79$, the volumetric fraction of H_2O in the flue gas can be estimated as

$$H_2O = \frac{(CO_2 + CO) \cdot CHR / 2 + N_2 \cdot R \cdot P_{sat} / (P_a \cdot 0.79) + m_S \cdot 22.4 / (18 \cdot V_d)}{1 + (CO_2 + CO) \cdot CHR / 2 + N_2 \cdot R \cdot P_{sat} / (P_a \cdot 0.79) + m_S \cdot 22.4 / (18 \cdot V_d)} \quad (4)$$

where P_{sat} is the saturation pressure of steam in the air.

Shown in Fig.3 is a comparison of the predicted dew points by using Eq.(4) and the measured ones with a capacitance-type humidity sensor. The measurement error of the dew points was ±2°C in the experimental condition. The calculated dew points by Eq.(4) agree well with the measurement.

The volumetric flow rate of wet gas, V_{wt}, is

$$V_{wt} = \frac{V_d}{1 - H_2O} \quad (5)$$

When the flue gas temperature is T_f°C, the steam mass concentration C_f per unit volume of flue gas is,

$$C_f = \frac{H_2O \cdot 18}{22.4} \cdot \frac{273.15}{273.15 + T_f} \tag{6}$$

The steam mass concentration W_f per unit mass of flue gas is

$$w_f = \frac{H_2O \cdot 18}{H_2O \cdot 18 + (1 - H_2O)(CO_2 \cdot 44 + CO \cdot 28 + N_2 \cdot 28 + O_2 \cdot 32)} \tag{7}$$

The steam mass concentration of the flue gas was controlled with injection of steam into the flue gas. The experimental conditions are shown in Tables.2.

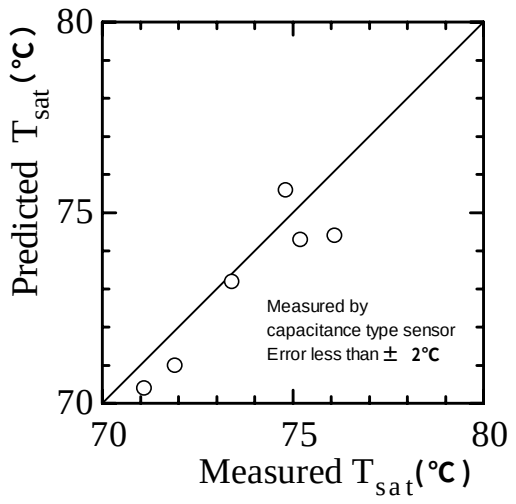

Fig. 3 Predicted and measured dew points

Table2 Test condition

Fin pitch (mm)	10mm	10mm	5mm	5mm
Air ratio μ	1.36	1.21	1.38	1.19
Flow rate V_{wt} (m_N^3/h)	201	239	213	244
Gas temp. T_f (℃)	121	124	112	124
Injected steam m_s (kg/h)	0	46	0	51
Steam conc. w_f (kg/kg)	0.106	0.263	0.101	0.279
Dew point T_{sat} (℃)	56.2	74.5	55.1	75.7
Re_f	11200	13300	12500	14100

3.2 HEAT TRANSFER CALCULATION OF FIN

The inner wall temperature of the polycarbonate test section was 85°C as a maximum. The contribution ratio of the radiation heat flux from the inner wall to the test tubes was within 5% of the total heat flux q_T when the emissivity of the polycarbonate wall and the tubes covered with the condensate were assumed as 1. As an accurate estimation of the radiation heat transfer is difficult, it was neglected in the following analysis. The total heat flux q_T consists of the convection heat flux q_V and the condensation heat flux q_C as

$$q_W = (q_V + q_C)(A_B + A_F\eta)/A_W \tag{8}$$

where A_W is defined as the heat transfer area when the fin height is 0. In the experiments, q_W was obtained from the temperature difference and flow rate of the cooling water. The convection heat flux is expressed as

$$q_V = h_V(T_f - T_w) \tag{9}$$

The condensation heat flux q_C can be expressed as,

$$q_C = h_C L_W (C_f - C_w) \tag{10}$$

The following empirical correlation[4] was available in the range of $2\times10^3 < Re_f \leqq 5\times10^5$.

$$Nu_f = j\,Re_f\,Pr_f^{0.33} \tag{11}$$

where

$$j = C_1 C_3 C_5 \left(\frac{d + L_F}{d}\right)^{0.5} \tag{12}$$

$$C_1 = 0.25\,Re_f^{-0.35} \tag{13}$$

$$C_3 = 0.35 + 0.65e^{-0.25L_F/S_F} \tag{14}$$

$$C_5 = 0.7 \tag{15}$$

The fin efficiency can be calculated by,

$$\eta = Y_F\left[0.45\ln\left(\frac{d + L_F}{d}\right)(Y_F - 1) + 1\right] \tag{16}$$

where

$$Y_F = X_F(0.7 + 0.3X_F) \tag{17}$$

$$X_F = \frac{\tanh(mb)}{mb} \tag{18}$$

$$m = \left[\frac{2h}{\lambda_F t_F}\right]^{0.5} \tag{19}$$

$$b = L_F + t_F/2 \tag{20}$$

The fin efficiency strongly depends on the heat transfer coefficient, h, in Eq.(19). These correlations were obtained from the single-phase experiment where the heat flux is a simple multiple of the constant heat transfer coefficient and the temperature difference between wall and fluid. Although the condensation heat flux can not be expressed with the above simple relation, it is considered that the Eq.(19) with the larger heat transfer coefficient taking account of the condensation heat transfer would give an approximation. As a first attempt, the following equivalent heat transfer coefficient in the condensation region was used.

$$h = h_V + \beta\frac{h_C L_W (C_f - C_W)}{T_f - T_W} \tag{21}$$

where β=1 for the usual calculation.

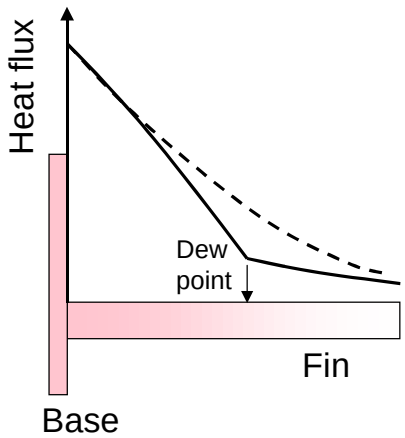

Fig. 4 Approximation of heat flux distribution

Shown in Fig.4 is a schematic image of heat flux distribution on a fin. The solid line depicts the heat flux distribution when the condensation takes place at the lower part of fin. As the dew point locates at the middle of fin, the heat flux sharply increases toward the base of fin from the dew point. The dash line is the calculated result with the equivalent heat

transfer coefficient of Eq.(21). The heat flux at the fin base is the same as the actual heat flux shown by solid line and the heat flux gradually decreases toward the fin tip without the effect of dew point. Generally the fin efficiency evaluated with Eq.(21) yields slightly the higher value than the actual one. However, at the white fuming condition when the saturation temperature merges with the gas temperature, the dew point never locate on the fin and the error due to the use of Eq.(21) becomes smaller.

For an analogous mass transfer, the simple analogy between heat and mass transfer gives,

$$Sh_f = j Re_f Sc_f^{0.33} \tag{22}$$

Flue gas was treated as a mixture of N_2, CO_2, O_2, CO and H_2O and its property was estimated with special combinations of each gas property proposed by the previous studies. For example, the heat conductivity and the viscosity were estimated with the methods by Lindsay&Bromley[5], and Wilke[6], respectively. It is considered that a strong relation exists between the thermal and mass diffusivities. As a first attempt, the mass diffusivity of steam in flue gas was estimated with the well-known mass diffusivity of steam in air as

$$D = D_{air}\left(\frac{\kappa}{\kappa_{air}}\right) \tag{23}$$

where κ and κ_{air} are the thermal diffusivities of flue gas and air, respectively. The diffusivity of steam in air[7] can be expressed as,

$$D_{air} = 7.65\times10^{-5}\,\frac{(T+273.15)^{11/6}}{P} \tag{24}$$

As it was difficult to install thermocouples on the fin surface, the base temperature of fin, T_W, was estimated from the average cooling water temperature T_L and the heat flux q_W. The maximum temperature difference, T_W-T_L, was 30℃ in the present experimental condition. The base temperature of fin is estimated as;

$$T_W = q_W d\left[\frac{\ln(d/d_i)}{2\lambda_S} + \frac{1}{\lambda_L Nu_L}\right] + T_L \tag{25}$$

where d: outer diameter of base tube, d_i: inner diameter. For the heat transfer of water-side, the correlation by Dittus-Boelter was modified to take into account the effect of inlet region. The coefficient by McAdams[8] was used for the modification as,

$$Nu_L = 0.023\,Re_L^{0.8}\,Pr_L^{0.4}\left(1+\left(\frac{d_i}{L}\right)^{0.7}\right) \tag{26}$$

where L is the heating length of tube. The heat conductivity for the inconel or austenite stainless steel is given with the following approximate correlation[9].

$$\lambda_S = 13.2 + 0.013T_S \quad W/(mK) \tag{27}$$

where T_S is the average temperature of base tube and defined as,

$$T_S = \frac{T_W + T_{Wi}}{2} \tag{28}$$

where T_W: outer wall temperature of base tube , T_{Wi}: inner wall temperature of base tube. The above estimation method was considered to be adequate from the comparison with the experiment of bare tubes without the fin[10].

3.3 EXPERIMENTAL RESULTS AND DISCUSSIONS

3.3.1 Fin tube of pitch 10mm

Shown in Fig.5 is a photograph when the temperature of base tube became approximately the dew point ($\triangle T_{sub}$= 0 K). The condensation behavior like fish-scales could be seen on the base tube between fins at around 45° from the tube top. However no condensation on the fin surface could be recognized.

Further decreasing the base tube temperature as the subcooling was $\triangle T_{sub}$= 8.5 K, the base tube was covered with a thin condensate film as shown in Fig.6. In this subcooling, no condensation on the fin surface could be recognized.

Shown in Fig.7 is a photograph when the subcooling became $\triangle T_{sub}$= 13.3 K. The base tube was almost covered with condensate but the most part of fin surface was still dry. The condensate flowed down and droplet of condensate was hanging on the fin of the lower part. So the temperature distribution of fin is not considered to be symmetric. It is possible that the re-evaporation takes place at the lower fin.

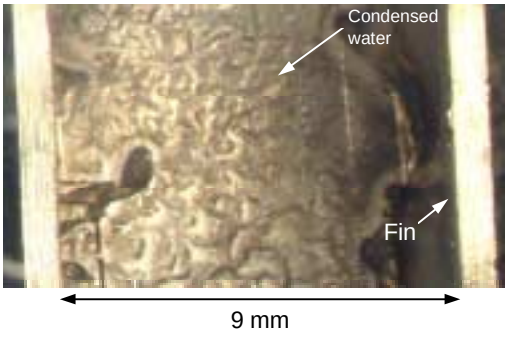

Fig. 5 Incipience of condensation ($\triangle T_{sub}$= 0 K)

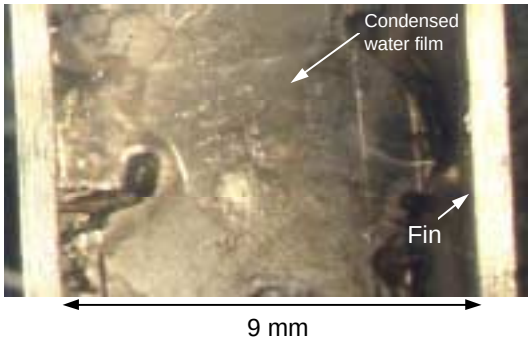

Fig. 6 Condensation behavior at $\triangle T_{sub}$= 8.5 K

Fig. 7 Droplet hanging on fin

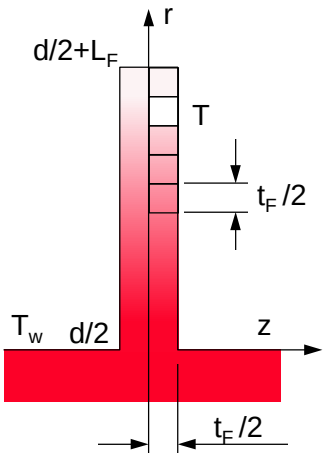

Fig. 8 Noding for numerical calculation of fin

When the symmetric temperature distribution on the circular fin is assumed, the distribution can be numerically obtained with the control-volume method[11]. The noding for the calculation is shown in Fig.8. Two nodings for Z direction and 24 nodings for the radial length are used. The heat conduction equation is

$$\frac{\partial^2 T}{\partial r^2}+\frac{1}{r}\frac{\partial T}{\partial r}+\frac{\partial^2 T}{\partial z^2}=0 \qquad (29)$$

When Re and temperature of flue gas is given, the heat flux is determined with the analogy correlation as a function of the wall temperature. The boundary conditions are

r= d/2 $\quad T=T_w$

r= d/2+L_F $\quad \lambda_F \frac{\partial T}{\partial r}=q_W(T)$

z= 0 $\quad \frac{\partial T}{\partial z}=0$

z= t_F/2 $\quad \lambda_F \frac{\partial T}{\partial z}=q_W(T)$

Shown in Fig.9 is calculation result for the radial temperature distribution in the fin of 10mm fin pitch varying the temperature of fin tip. The temperature gradient is steep below the dew point indicating the high heat flux due to the condensation. Even when the base tube temperature decreases below the dew point, the tip temperature is approximately 90℃. When the base temperature further decreases to 0℃, the tip temperature is approximately 70℃ and much higher than the dew point. These supports the observation result that the most part of fin surface was dry when the condensation at the base tube initiated.

The fin efficiency can be obtained from the numerically calculated temperature distribution as

$$\eta=\frac{\int_{d/2}^{d/2+L_F} q_w(T)2\pi r dr+\left[q_w(T)\right]_{r=d/2+L_F}\pi(d/2+L_F)t_F}{q_w(T_w)\pi\left\{(d/2+L_F)^2-d^2/4+(d/2+L_F)t_F\right\}} \qquad (30)$$

The fin efficiency also can be obtained experimentally from the experimental heat flux $[q_w]_{exp.}$ with the following equation,

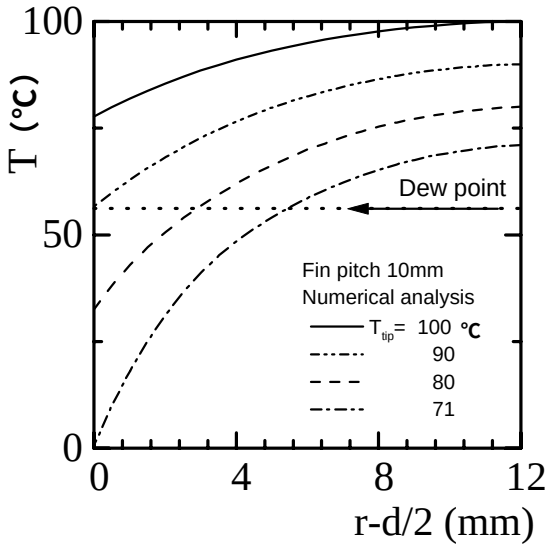

Fig. 9 Temperature distributions in fin

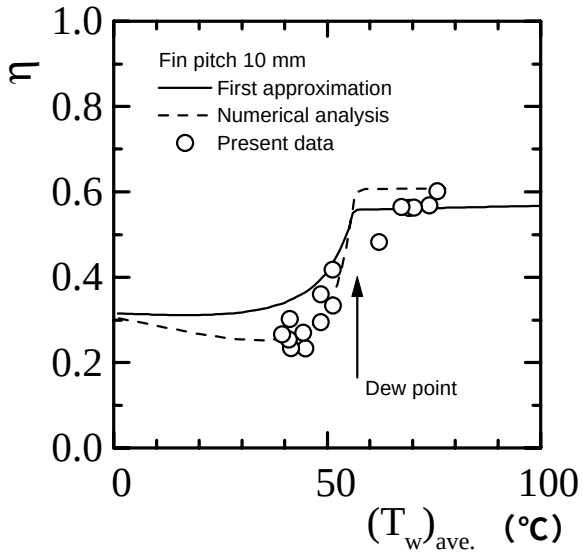

Fig. 10 Fin efficiency at pitch of 10mm

$$\eta=\frac{[q_w]_{exp.}A_W-q_w(T_w)A_B}{A_F q_w(T_W)} \qquad (31)$$

Shown in Fig.10 is the relation of experimental fin efficiency and the average temperature of base tube comparing with those obtained from the numerical calculation and the first order approximation. In the first order approximation, the equivalent heat transfer is used to evaluate the fin efficiency in the empirical correlation of Eq.(16). Increasing the base tube temperature, the experimental fin efficiency sharply drops at the dew point. This behavior is considered to be due to the fact that a large amount of heat flows in the fin and the temperature difference between the fin tip and bottom becomes large when the condensation takes place. The experimental efficiency agrees well with that obtained with the numerical calculation assuming the symmetrical heat flow in the fin. The asymmetric temperature distribution at the lower fin observed in the above photographs does not have a significant effect on the total fin capability. However it is possible that the re-evaporation at the lower fin condenses the condensate and leads to the severe

erosion.

Shown in Fig.11 is the relation between the total heat flux and the average base tube temperature of fin tube of pitch 10mm with and without steam injection. The steam mass concentration w_f was 0.106 without steam injection and increased to 0.263 with the steam injection of 46 kg/h. The corresponding dew point increased from 56.2°C to 74.5°C. The solid lines predicted by the simple analogy correlation agree well with the experimental heat flux with and without steam injection.

3.3.2 Fin tube of pitch 5mm

The same condensation behavior was also observed in the fin of pitch 5mm. Due to the narrow fin pitch, the water bridge between the lower fin was observed as shown in Fig.12. The photograph was taken at the base tube subcooling of $\triangle T_{sub}$= 0.3 K. Asymmetric temperature distribution is also suggested in the photograph as same as that in the fin tube of pitch 10mm.

Shown in Fig.13 is the relation of experimental fin efficiency and the average temperature of base tube comparing with those obtained from the numerical calculation and the first order approximation. Increasing the base tube temperature, the experimental fin efficiency sharply drops at the dew point of 55.9°C. The experimental efficiency agrees well with that obtained with the numerical calculation assuming the symmetrical heat flow in the fin. The asymmetric temperature distribution at the lower fin observed in the above photographs does not have a significant effect on the total fin capability.

Shown in Fig.14 is the relation between the total heat flux and the average base tube temperature of fin tube of pitch 10mm with and without steam injection. The steam mass concentration w_f was 0.101 without steam injection and increased to 0.279 with the steam injection of 51 kg/h. The corresponding dew point increased from 55.1°C to 75.7°C. The solid lines predicted by the simple analogy correlation agree well with the experimental heat flux with and without steam injection.

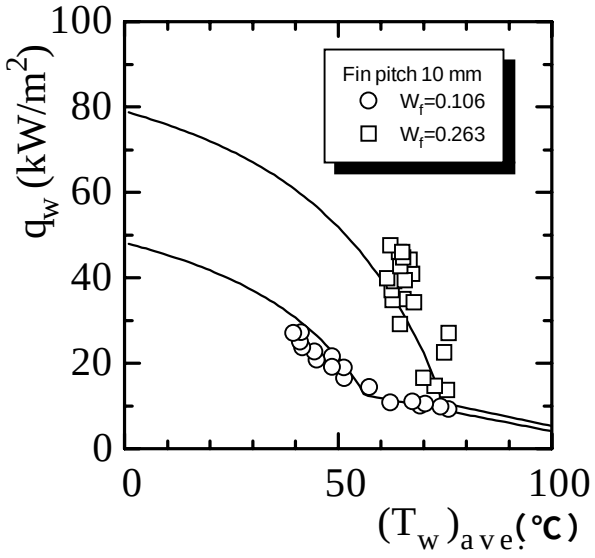

Fig. 11 Relation between heat flux and average base tube temperature of fin tube of pitch 10mm.

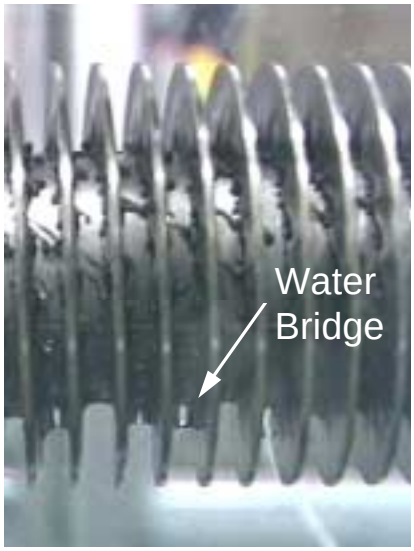

Fig. 12 Water bridge between the fins

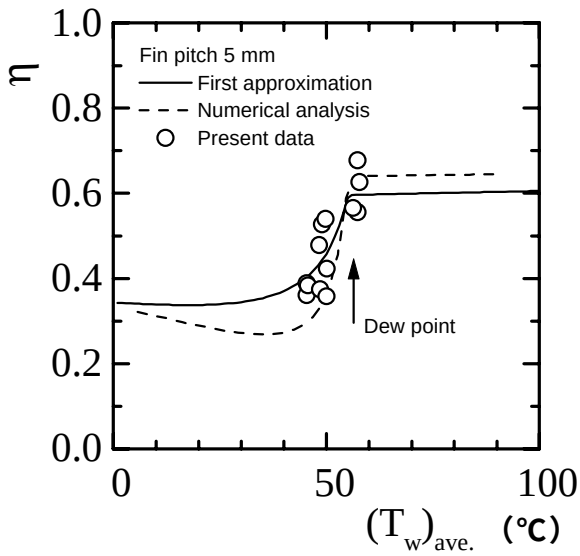

Fig. 13 Fin efficiency at pitch of 5mm

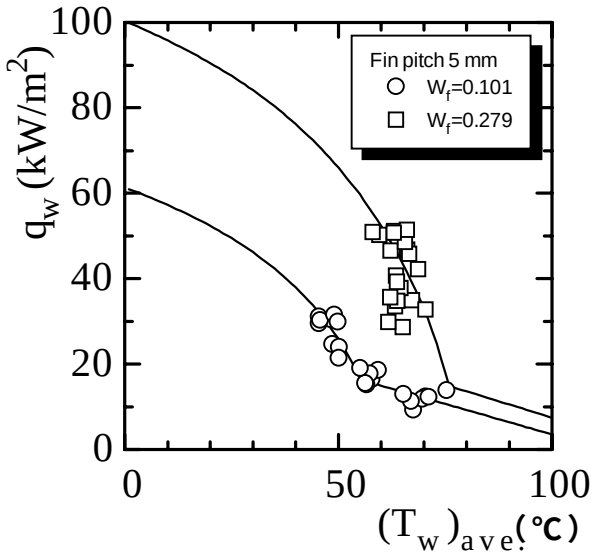

Fig. 14 Relation between heat flux and average base tube temperature of fin tube of pitch 5mm.

4. ECONOMIZER EXPERIMENT

4.1 EXPERIMENTAL APPARATUS AND METHOD

Shown in Fig.15 is a schematic of experimental apparatus. The flue gas from a propane gas boiler is led to the lower plenum and flows upward and downward through the bank of tubes. The flue gas was released to atmosphere from the outlet plenum. Three kinds of countercurrent cross-flow heat exchangers, which consist of bare tubes, spirally finned tubes of fin pitch 5 and 10mm, were designed and used for the experiment. The length of the bare and finned tubes was 482mm. The temperature distributions of water and flue gas in the heat exchanger were measured with sheath K-type thermocouples of 1.6 mm in diameter. The thermocouple signals were transferred to a personal computer with a GPIB line and analyzed. The measurement error of the temperature in this study was within ±0.1 K. The pressure loss and the total amount of condensate generated in the heat exchanger were also measured.

Shown in Fig.16 is the arrangement of heat transfer tubes. The heat exchangers of finned tubes consist of staggered banks of 3-2 rows, 34 stages for the fin pitch 10mm and 20 stages for the pitch 5mm. The detail of the finned tube is already shown in Fig.2. The outer and inner diameters of the base tube installed with the fins are 34 and 28.8mm, respectively. The thickness and height of the plate fin are 1 and 12mm, respectively. The parametric study varying the flue gas flow rate, feed water temperature and flow rate was conducted. The experimental conditions for the finned tube experiments are shown in Tables.3. In a part of the finned tube experiments of fin pitch 5mm, spacer rods of 23 mm in diameter were inserted in the tubes to increase the water velocity.

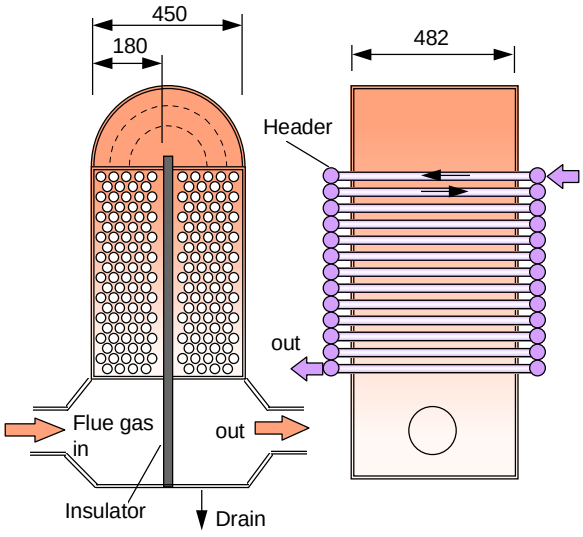

Fig. 15 Schematic of experimental apparatus

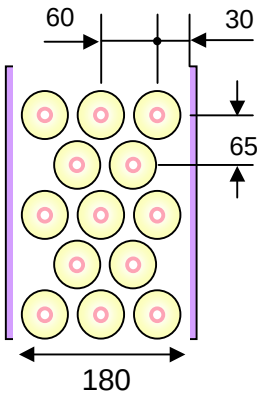

Fig. 16 Arrangement of heat transfer tubes

Table3 Test conditions of finned tube

Test no.	p10-1	p10-3	p10-4	p5-1	p5-4	p5-6
Fin pitch (mm)	10	10	10	5	5	5
Spacer rod	No	No	No	No	Yes	Yes
Air ratio μ	1.17	1.18	1.34	1.18	1.16	1.15
Fuel flow rate (m_N^3/h)	18.9	19.3	11.9	18.8	18.8	18.7
Gas inlet temp. (℃)	190	198	186	193	190	191
Feed water (kg/h)	630	1202	630	630	633	1207
Water inlet temp. (℃)	14.7	15.1	15.1	14.8	29.3	29.9

Table4 Composition of Propane gas fuel

C_3H_8	98 %
C_4H_{10}	2

4.2 EXPERIMENTAL RESULT AND PREDICTION

4.2.1 Temperature distribution in bank of fin pitch 10mm tubes

Shown in Fig. 17 is the comparison of experimental result and one-dimensional prediction for the bank of fin pitch 10mm tubes. The outer wall temperature for the finned tube depicts the outer wall temperature of the base tube where the fins are welded. As it was difficult to avoid the falling condensate on the thermocouples in the finned tube configuration, the thermocouple signal sometimes indicated the lower temperature than the actual gas temperature. The scattering of the gas temperature is considered to be due to the wet thermocouples. The gas temperature locally rises as much as 20°C at the middle of the bank where the gas flow becomes the down-flow from the up-flow. It is considered that the thermocouple indicates the correct gas temperature at the middle position as it locates enough above the condensing bank. It should be noted that the measured gas temperature with the dry thermocouple agrees well with the predicted gas temperature. The general temperature profiles can be predicted well with the one-dimensional mass and heat balance calculation.

The above mentioned study for the single stage showed that the condensate flowed downward and re-evaporated on the lower part of fin. It is possible that the re-evaporation takes place more frequently in the multiple stage as the condensate generated at the upper stage falls down on the lower stage. The re-evaporation decreases the net heat flux from gas to water. So the parametric calculation for the fin efficiency was conducted. When β=5 was used in the Eq.(21), the fin efficiency became approximately the half of that at β=1 at the condensing region. However, the significant difference could not be observed on the general behavior. The lower fin efficiency decreases the outer wall temperature of the base tube welded with fin. So the condensation heat transfer coefficient increases significantly with the decreased wall temperature. As the result, the net heat flux from the gas to the water can not be affected significantly with the fin efficiency in the condensing region. In the non-condensing region, the heat transfer coefficient is not affected with the wall temperature and the net heat transfer decreases significantly with a decrease of the fin efficiency. It is considered that the degraded fin efficiency in the condensation region does not have a strong effect on the general calculation result.

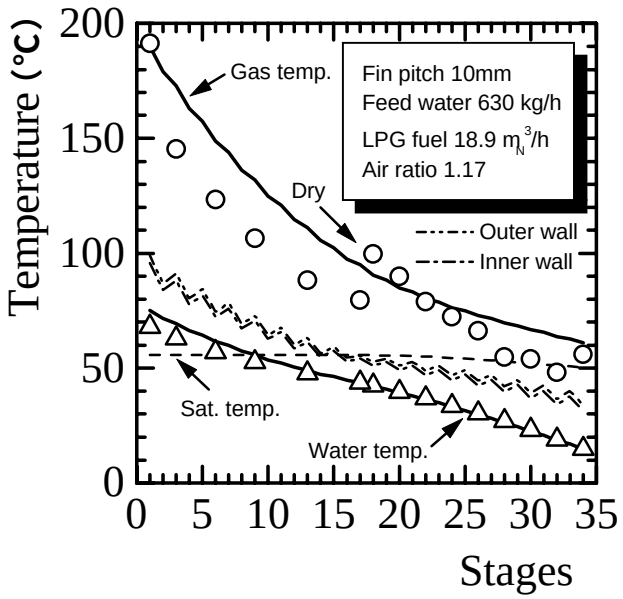

Fig. 17 Finned tube experiment at feed water flow rate of 630kg/h and fuel flow rate of 18.9m$_N^3$/h

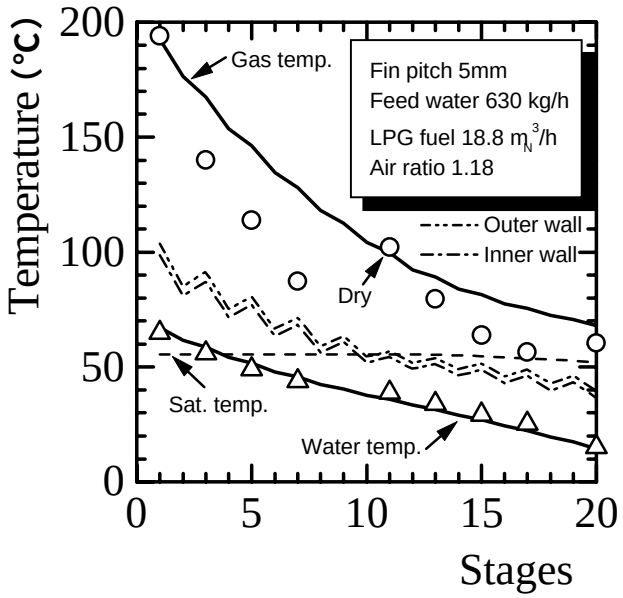

Fig. 18 Finned tube experiment at feed water flow rate of 630kg/h and fuel flow rate of 18.8m$_N^3$/h

4.2.2 Temperature distribution in bank of fin pitch 5mm tubes

Shown in Fig. 18 is the comparison of experimental result and one-dimensional prediction for the bank of fin pitch 5mm tubes. The scattering of the gas temperature is also considered to be due to the wet thermocouples. The measured gas temperature with the dry thermocouple at the middle of bank agrees well with the predicted gas temperature. The general temperature profiles can be predicted well with the one-dimensional mass and heat balance calculation.

5. CONCLUSION

(1) Condensation heat transfer on horizontal spirally finned tubes of fin pitch 5 and 10mm was investigated experimentally by using an actual flue gas from a natural gas boiler. The experiments were conducted at different steam mass concentrations of the flue gas and a wide range of tube wall temperature. The mass concentration was controlled with a steam injection into the flue gas. Fin efficiency at the condensation region was significantly lower than that at the dry region. The empirical correlation developed for a single-phase fluid was extrapolated to the condensation heat transfer region. The fin efficiency was evaluated with an equivalent heat transfer coefficient used as a first approximation. The heat and mass transfer behaviors on the spirally finned tube were well predicted with the analogy correlation based on the empirical correlation.

(2) Thermal-hydraulic behavior of the economizer for the latent heat recovery was investigated experimentally by using an actual flue gas from a propane gas fuel boiler. The above mentioned correlation was incorporated into the prediction code and verified with the experiments. The experimental results for the temperature distributions of water and flue gas in the test heat exchangers with bare and finned tubes agreed well with the prediction.

ACKNOWLEDGMENT

The authors appreciate the helpful supports by Miura Institute, Miura Industry Co. Ltd., The Japan Society of Industrial Machinery Manufacturers and NEDO (New Energy and Industrial Technology Development Organization of Japan).

REFERENCES

(1) Taniguchi, H., Kudo, K., Huang, Qi-Ri and Fujii, A., 1987, "Heat mass transfer from air with high water content(latent heat recovery from flue gas)", (in Japanese) *Trans. of JSME*, 53-495, B, 3377-3382

(2) Kanzaka, M., Soda, M., Yokoo, K., Iwabuchi, M. and Osada, I., 1992, "Recovery of water from flue gas(heat and mass transfer on the spirally finned tube)", (in Japanese), *Trans. of JSME* , 58-545, B, 248-253

(3) Kawamoto, K., Nagane, K. and Ohashi, Y., 1995, "Investigation on the latent heat recovery from flue gas", (in Japanese), *Proc. of 32nd Heat Transfer Symposium of Japan*, G142

(4) ESCOA FINTUBE CORPORATION, 1979, SOLIDFIN HF.

(5) Lindsay, A.L. and Bromley L.A., 1950, "Thermal conductivity of gas mixtures", *Indust. Engng. Chem.*, 42, 1508-1510.

(6) Wilke, C.R., 1950, "A viscosity equation for gas mixture", *J. Chem. Phys.*, 18, 517-519.

(7) Fujii, T., Kato, Y and Mihara, K., 1977, "Expressions of transport and thermodynamic properties of air, steam and water", *Univ. Kyushu Research Institute of Industrial Science Rep.*66, 81-95.

(8) McAdams, W.H., 1954, *Heat transmission*, McGRAW-HILL.

(9) Osakabe, M., 1989, "Thermal-hydraulic study of integrated steam generator in PWR", *J. Nucl. Sci. & Technol.*, 26(2), 286-294.

(10) Osakabe, M., Yagi, K., Itoh, T. and Ohmasa, M., 1999, "Condensation heat transfer on tubes in actual flue gas (Parametric study for condensation behavior)", (in Japanese), *Trans. of JSME* , 65-632, B, 1409-1416.

(11) Patankar, S.V., Numerical Heat Transfer and Fluid Flow, Hemisphere P.C., (1980)